Development of an Aerogel-Based Wet Electrode for Functional Electrical Stimulation

Melissa Marquez-Chin, Zia Saadatnia, Hani E. Naguib, and Milos R. Popovic

***Abstract*— Functional electrical stimulation (FES) has been a useful therapeutic tool in rehabilitation, particularly for people with paralysis. To deliver stimulation in its most basic setup, a stimulator and at least a pair of electrodes are needed. The electrodes are an essential part of the system since they allow the transduction of the stimulator signals into the body. Their performance can influence the experience of both patient and therapist in terms of movement generation, comfort, and ease of use. For non-invasive surface stimulation, current electrode options have several limitations involving their interfacing with the skin, practical inconveniences, and short-term functionality. Standard hydrogel electrodes tend to lose their adhesion with the skin quickly, while dry or textile electrodes require constant wetting to be comfortable. In this paper, we present the fabrication, characterization, and FES testing of a new aerogel-based wet electrode for surface stimulation applications for long-term and reusable FES applications. We investigated its functionality by stimulating the biceps brachii of twelve healthy individuals and collected elbow joint torque and comfort ratings for three different intensity levels (low, moderate, and high) of FES. Comparing to standard hydrogel electrodes, no statistically significant difference was found for any intensity of stimulation in either torque or comfort. Overall, the new aerogel-based electrode has an appropriate impedance, is flexible and soft, is conformable to the skin, has a high water absorption and retention, and can be used for FES purposes.**

***Index Terms*— Aerogel-based electrode, comfort, functional electrical stimulation, reusable electrode, torque.**

Manuscript received 19 April 2023; revised 10 September 2023; accepted 4 October 2023. Date of publication 13 October 2023; date of current version 20 October 2023. This work was supported in part by the Natural Sciences and Engineering Research Council, in part by the Walter and Maria Schroeder Foundation, and in part by the National Council of Science and Technology of the United Mexican States Graduate Scholarship. *(Melissa Marquez-Chin and Zia Saadatnia are co-first authors.) (Corresponding author: Melissa Marquez-Chin.)*

This work involved human subjects or animals in its research. Approval of all ethical and experimental procedures and protocols was granted by the University Health Network's Research Ethics Board under Application No. 21-5298, and performed in line with the Declaration of Helsinki.

Melissa Marquez-Chin and Milos R. Popovic are with the Institute of Biomedical Engineering, University of Toronto, Toronto, ON M5S 3G9, Canada, and also with the KITE—Toronto Rehabilitation Institute, University Health Network, Toronto, ON M5S 3G9, Canada (e-mail: melissa.marquezchin@mail.utoronto.ca; milos.popovic@uhn.ca).

Zia Saadatnia is with the Department of Mechanical and Manufacturing Engineering, Ontario Tech University, Oshawa, ON L1G 0C5, Canada, also with the Department of Mechanical and Industrial Engineering, University of Toronto, Toronto, ON M5S 3G8, Canada, and also with the KITE—Toronto Rehabilitation Institute, University Health Network, Toronto, ON M5S 3G9, Canada (e-mail: zia.saadatnia@ontariotechu.ca).

Hani E. Naguib is with the Department of Mechanical and Industrial Engineering, University of Toronto, Toronto, ON M5S 3G8, Canada, and also with the KITE—Toronto Rehabilitation Institute, University Health Network, Toronto, ON M5S 3G9, Canada (e-mail: naguib@mie.utoronto.ca).

This article has supplementary downloadable material available at https://doi.org/10.1109/TNSRE.2023.3324400, provided by the authors.

Digital Object Identifier 10.1109/TNSRE.2023.3324400

I. Introduction

FUNCTIONAL electrical stimulation (FES) consists of delivering electrical pulses to produce muscle contractions which can be used for rehabilitation of people with paralysis [1], [2], [3]. These pulses are delivered through electrodes which become the main interface between the stimulator and a patient. Electrodes can be placed on the top of the skin (i.e., transcutaneous), through the skin (i.e., percutaneous), directly on the nerve (i.e., cuff), or directly on the muscle next to the nerve (i.e., epimysial) [1], [2]. Their charge transfer can be influenced by many factors, including placement, the skin-electrode interface, the electrode material, and the stimulator used, which can ultimately affect movement production and comfort sensations during stimulation [4], [5], [6], [7]. These factors can also play a role in the user's experience, being it the patient or the therapist.

Transcutaneous electrodes have the benefits of being non-invasive and easy to apply and remove. The types of transcutaneous electrodes used to date include sponge electrodes, carbon rubber electrodes, hydrogel electrodes, and textile electrodes [5]. One of the most commonly used type of transcutaneous electrode is the self-adhesive hydrogel electrode. Their wide use is understandable given their non-invasive nature and easy application. They consist of multiple layers of material which include an adhesive gel that allows it to adhere directly to the skin [5]. These types of electrodes, however, have the disadvantage of degrading after multiple uses making it lose its adhesive properties quickly. In order to keep the electrodes in place, an elastic bandage or other additional supports can be wrapped around the electrode. This prevents the electrodes from falling off due to body movement, tugging on the cable connecting the electrode to the stimulator, or the weight of the cable connecting the electrode to the stimulator. Hydrogel electrodes are also not reusable, which makes them more expensive to use if multiple sessions are needed. Recently, textile electrodes have been proposed as a solution for some of the hydrogel electrodes limitations, however they require constant wetting in order to

be comfortable, which makes them not as viable solution as the hydrogel electrodes [8], [9], [10], [11].

Aerogels are nano-porous materials with ultra-high porosity where the solid content of the aerogel structure can be as low as 5% of the total volume of the material [12]. An aerogel can be targeted as a novel biomedical electrode by: i) the use of biocompatible, washable, and water absorbent materials to fabricate the aerogel electrode, ii) the addition of electrical conductivity into the solid porous structure, and iii) including water in the nano-porous structure of the aerogel by filling the pores with water [13]. For electrical stimulation applications, the porosity of the aerogels could be exploited to create an advanced stimulation electrode by filling >90% of the volume of empty space with water, which is an ideal medium that would enable flow of charges between the electrode and the skin tissues. If the aerogel structure is formed by a hydrophilic material, it would be able to retain that large amount of water. The high-water content would also result in the conductivity being minimally affected by humidity and sweating. This provides a wet environment at the electrode-skin interface for the delivery of a smooth stimulation for extended periods of time. The conductive solid structure of the aerogel can provide the essential electrical conductivity for the stimulation, and the washable and hydrophilic properties of the material can ensure the repetitive wettability and usability of the electrode. Here, we propose to use cellulose as the main component of the aerogel with multi-walled carbon nanotube (CNT) as conductive fillers to add electrical conductivity through the solid structure. Cellulose has high water absorption capability, biocompatibility, and the ability to form a gel and to construct the porous structure. CNTs have high surface area, electrical conductivity, and chemical stability. We have characterized these electrodes, and analyzed the effects of the conductive filler and fiber on the mechanical and electrical properties. We have also tested these new electrodes during FES and compared their performance to standard hydrogel electrodes in terms of torque production and comfort scores. In this study, we show that the proposed aerogel-based electrode has a high-water content and retention, is soft and flexible, has a low impedance, can be used multiple times, and can be used for FES.

II. Materials and Methods

A. Materials for Electrode Fabrication

Multi-walled Carbon Nanotube (CNT-NC7000) was obtained from Nanocyl (Belgium) where the carbon nanotubes have the average diameter of 9.5 nm, average length of 1.5 μm, surface area of 25-300 m^2/g, and volume resistivity of 10-4 Ω·cm on powder. Sodium Hydroxide (NaOH) was supplied by CALEDON Laboratory Chemicals (Canada). Urea was obtained from BioShop Life Science Products (Canada). Dimethylformamide (DMF), Poly(diallyldimethylammonium chloride) (PDDA) solution (20 wt% in water), N,N'-methylenebis(acrylamide) (MBA), and cellulose powder (medium size, cotton linters) were purchased from Sigma-Aldrich (USA). Ethanol was purchased from University of Toronto Chem Stores (Canada). Polyvinylidene Fluoride (PVDF, Kynar 740) and Neoprene rubber sheet (40A-medium soft) were supplied from Arkema (Canada) and McMaster-Carr (Canada), respectively. Agar-agar powder was obtained from Landor Trading Company (Canada). All materials were used without any further purification. Deionized (DI) water was used for all experiments.

B. Fabrication of the Electrodes

Aerogels can be fabricated through very specific procedures requiring high-precision control of the selection of materials and the fabrication process. Generally, an aerogel is made by two main consecutive steps: the formation of a relatively hard gel from the dissolved solid compounds with a large amount of liquid content trapped inside the porous solid structure, and then replacing the liquid content with air without collapsing the solid structure by means of a controlled drying procedures such as freeze-drying and super-critical (SC) drying [14]. For the aerogel-based wet electrodes, we replaced the liquid content of the gel with water and filled up the porous structure with water to obtain the wet electrode. The detailed fabrication process is explained below.

The fabrication process of the aerogel-based wet electrode is schematically shown in Fig. 1. A low-cost and green solvent was required for dissolving cellulose based on a standard alkali solution composed of water, Urea, and NaOH [15]. However, first we needed to uniformly disperse CNT into water and then add other chemicals to prepare the solvent for breaking down the cellulose. We prevented CNT agglomeration and sedimentation, and created uniform dispersion of CNTs in water by using surfactants like PDDA [16]. Accordingly, water (81 wt% of the solvent), PDDA (1 wt% of water), and CNT (2-6 wt% of cellulose) were added together and mixed by ultra-sonication for 1 hr under 50 Watts. The mixture was kept inside a water bath during the sonication to lower the temperature rise due to the sonication process. After obtaining a uniform dispersion of CNT in water, we added NaOH (7 wt% of the solvent) and Urea (12 wt% of the solvent) and mixed it by a magnetic stirrer for 30 min at room temperature to fully dissolve the NaOH and Urea. This provided a green water-based solvent to break down and then stabilize the cellulose broken chains [15]. With the solvent prepared, we gradually added cellulose powder (5 wt% of the total solution) and mixed it by a magnetic stirrer for 30 min at room temperature. The small amount of cellulose kept the solid content very low and obtained a high porosity through the final electrode structure. Note that at this stage, the cellulose was only dispersed into the solvent as it could not be dissolved at room temperature. The solution was then transferred into a freezer and kept at <-15 °C for at least 12 hrs. Cooling down the solution allowed the solvent to fully dissolve the cellulose and stabilize the broken polymer chains through the solution [15]. Then, the total solution was removed from the freezer and by vigorously mixing at room temperature for 5-10 min, we obtained a fully dissolved cellulose compound with a full entanglement with CNT nanoparticles which have already been dispersed in the solution. To form the initial gel, we then added the chemical crosslinking agent MBA (1.5 wt% of water) into the solution [17]. Then by mixing with a magnetic stirrer at room temperature for 3 hrs, we ensured the full dissolution of the

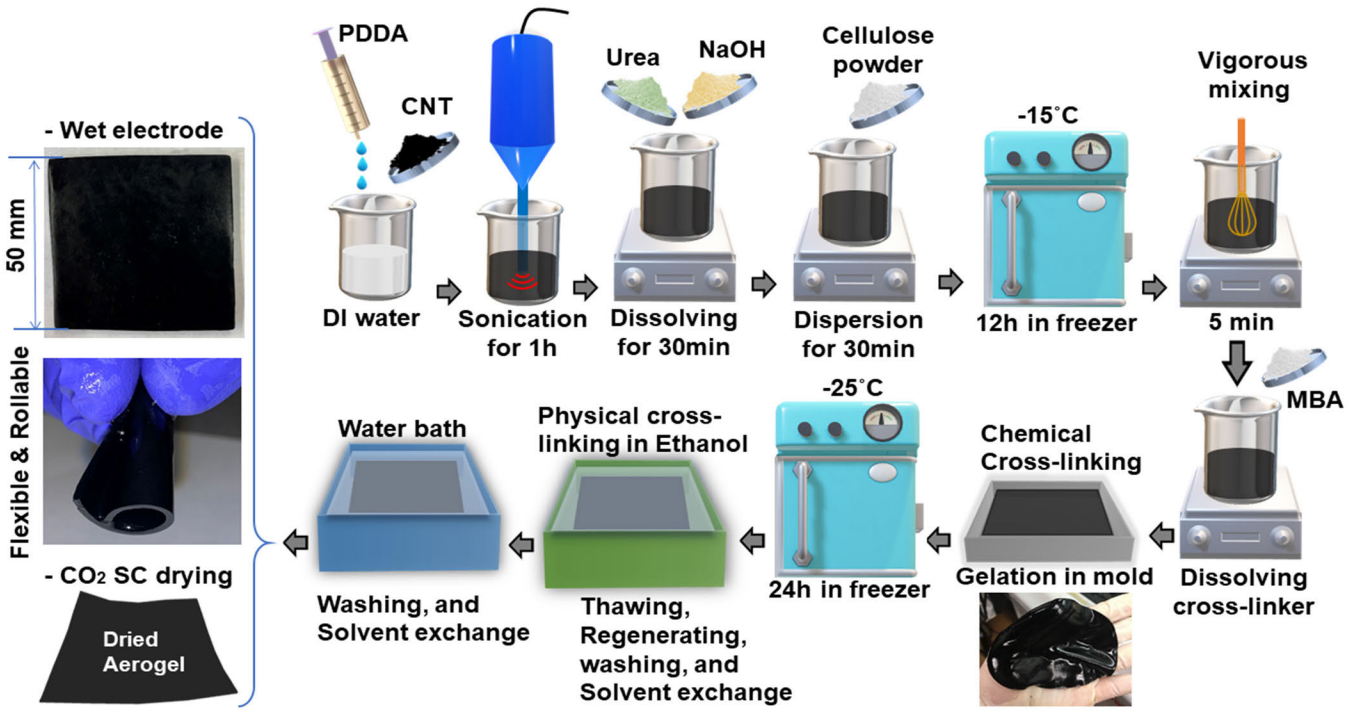

Fig. 1. Fabrication process of the aerogel-based wet electrode for the FES application.

MBA. Once the MBA was dissolved, the solution was casted into customized Teflon molds to form a gel in the desired film shape. The samples were left at room temperature for 4-5 hrs to let the chemical cross linker work and to form the initial soft gel. Then, the molds holding samples were transferred into a freezer <-25 °C for at least 24 hrs. This allowed the liquid content of the gels to become frozen and hold their shape avoiding shrinkage in the next step, i.e., the physical crosslinking. The frozen samples were then soaked into an ethanol bath for physical crosslinking and the formation of a relatively hard gel. If the samples were not frozen, they would shrink and curve up quickly once soaked into ethanol. The samples need to remain in ethanol for 6-8 hrs, and we exchanged the ethanol with fresh ethanol every 2 hrs during this step. Ethanol acted as a regenerating chemical causing the physical crosslinking of the polymer composite structure, which improved the mechanical properties and the uniform formation of regenerated cellulose [15]. The regeneration process was due to the repulsion between cellulose material and ethanol resulting in a stronger entanglement and bonding between the polymer chains as a physical crosslinking method. Ethanol also removed undissolved or unreacted compounds of the samples when the liquid content inside the gel was exchanged with the ethanol in the bath due to the open-cell porous structure of the gels. This process, also known as solvent exchange and washing, was a very important step which justified the need for frequently exchanging the ethanol with fresh ethanol for a more effective process. The gels formed a relatively hard structure which could be easily removed from the molds and cut into desired shapes and dimensions. At this stage, the ethanol filled the majority of the open–cell content of the formed gels.

A small portion of the gel samples were used for the super critical (SC) drying process. This process could remove the liquid content of the gel without collapsing the solid structure and gave us a dry nano-porous aerogel which was necessary for the characterizations requiring dry samples. The SC drying was performed by a super-critical fluid like CO_2 and it required the liquid content of the gel to be highly soluble in CO_2 [14]. Ethanol filled the open-cell content of our prepared samples so we could successfully dry our samples by the SC drying process to obtain the aerogel for characterization purposes. Note that this process could not be performed on the gels originally filled with the water-based liquid due to the very low solubility of water in CO_2. A freeze-drying process could be performed for drying water-filled gels instead, but it could enlarge the porosities inside the aerogel structure due to water expansion when freezing into ice, which was not desired for our design [18].

The other portion of the formed gels with the desired shapes was soaked into a water bath to exchange the ethanol with water. This step exchanged the ethanol in the porous structure with water and washed away any unreacted components left from the previous steps. The samples needed to remain in water for at least three weeks and the water in the bath had to be exchanged with fresh water every 24 hrs for the first week and every three days for the rest of the process. After that, we obtain the conductive and wet aerogel-based electrode with a high-water content trapped inside the porous solid structure. The wet electrode showed a high flexibility due to hydrophilicity of the cellulose matrix and no repulsion between cellulose and water as well as a desired structural integrity due the completed two-step cross-linking process. This allowed for the testing of the fabricated wet electrodes

in the FES application. The fabricated aerogel-based sample electrode (~ 2 mm thick) is presented in Fig. 1.

C. Electrode Characterization

1) Morphology Inspection: To explore the morphology and the micro-porous open-cell structure of the fabricated electrodes, the super-critical (SC) dried electrode was tested by a scanning electron microscope (SEM- JSM-IT100 InTouchScope), as shown in Fig. 2(a)-(c). A typical sample with 4wt% CNT concentration was selected for this measurement. Fig. 2(a) shows the cross-section of the electrode in a lower magnification to represent the overall distribution of the micro pores through the structure of the developed material. The higher magnification of the porous structure is shown in Fig. 2(b) where the approximate sizes of the pores as well as the open-cell configuration of the pores were observed. It is also very important to show the micro-structure assembly of the pores at the edge of the electrode when looking into the cross-section of the film material. This is useful to explore any skinning effect where the structure is susceptible to show less porosity near the surface by having more solid structure and higher density which may affect the properties of the material such as dielectric or conductivity properties [19]. Fig. 2(c) shows the cross-section of the dried sample at the near edge in which it is evident that no significant dense layer was observed adjacent to the surface of the material and the pores distribution remained almost the same as the inner side representing a homogenous structure throughout the material.

2) Chemical Characterization: The chemical characterization of the fabricated electrodes was performed by means of Fourier transform infrared (FTIR) spectroscopy (Bruker ALPHA system, USA) for realizing the formation of cellulose polymeric matrix as well as the role of chemical cross-linking agent (MBA), as shown in Fig. 2(d). The FTIR test on the SC dried electrode material showed the typical bands related to cellulose formation including the characteristic peaks of 895 cm^{-1}, 1063 cm^{-1}, 1160 cm^{-1}, 2899 cm^{-1}, and 3350 cm^{-1} confirming the construction of a cellulose matrix [20]. The characteristic peaks at 1545cm^{-1} and 1657cm^{-1} bands belong to the –NH flexural vibration absorption and –C=O stretching vibration absorption of the MBA which are clearly found in the FTIR spectrum of the electrode material showing the incorporation of the MBA for crosslinking the cellulose polymer chains [20]. Moreover, it was reported in the literature that the FTIR spectrum of non-reacted MBA should also show characteristic peaks at 1620 cm^{-1} and 3067 cm^{-1} corresponding to –C=C–H and C=C bands, respectively [17]. However, these bands were not observed in the spectrum of the fabricated electrode referring to their consumption during the cross-linking process [17]. Overall, the FTIR results validated the successful formation of the polymer matrix and chemical crosslinking through the structure of the fabricated electrode material.

3) Tensile Strength: The mechanical behavior of the wet electrode was analyzed by performing tensile test on the film samples by means of a Dynamic Mechanical Analyzer (DMA, Q800, TA Instrument, USA). The tensile stress-strain responses of the wet film electrodes were extracted considering the effect of the concentration of CNT conductive filler in the electrode material. Accordingly, three samples were tested namely S1, S2, and S3 corresponding to 2wt%, 4wt%, and 6wt% CNT concentration, respectively. The stress-strain curves of the three samples are shown in Fig. 2(e). The effect of the CNT concentration on the tensile modulus, yield strength, and tensile strength of the wet electrodes is clearly observed in the stress-strain results. The material's tensile modulus, which corresponds to the slope of the first linear region of the curves, significantly increases by the CNT amount. The approximate tensile modulus of 0.18 MPa, 0.62 MPa, and 1.15 MPa were calculated for S1, S2, and S3 samples, respectively. These values were within the range of the tensile modulus of human skin where S2 owns the closest tensile modulus to human skin [21]. The flexibility and softness of the wet electrodes could be attributed to the porous structure, the presence of water content, and the hydrophilic and swelling properties of cellulose [22]. The yield strength (i.e., the stress in which the curves transform to the nonlinear plastic region), and the tensile strength (i.e., the stress where the material fails) were both increased by the CNT concentration. Such effect of CNT filler on the mechanical properties of the developed material was expected as the CNT with ultra-high stiff and strong mechanical properties is a well-known additive in polymer composites for improving the stiffness and strength of composite materials [23].

4) Electrical Characterization: To measure the electrical properties of the wet electrodes, the impedance of the developed material was measured for three CNT concentrations including Sample 1 (2 wt%), Sample 2 (4 wt%), and Sample 3 (6 wt%) where the wt% was counted with respect to the cellulose content. For this purpose, we used an electrochemical analyzer (Model CHI6054E, CH Instruments, USA) with the electrochemical impedance spectroscopy (EIS) technique [24]. The experimental setup consisted of a three-electrode configuration with a saturated calomel (Hg_2Cl_2) electrode as the reference electrode, a platinum electrode as the counter electrode, and a square sample (2 cm x 2 cm) of the developed material as the working electrode. The electrolyte used was 0.9% saline solution at room temperature. A schematic on the experimental setup used can be found in Fig. S1. The three electrodes were placed in a cylindrical plastic container filled with the solution. The parameters used were a sine wave with an amplitude of 0.5 V (peak-to-peak) and a frequency range from 0.1 Hz to 10 kHz. This procedure was performed for the three different samples of the material after being soaked in water. The resulting curves from the EIS measurements can be seen in Fig. 3.

All three samples showed a relatively similar electrical behaviour as seen in the magnitude and phase responses in Fig. 3. The variation in performance can be attributed to the solution's dominance over the electrical properties in the samples with lower CNT percentage. The samples also showed a minimally variant impedance magnitude and phase as shown in Table I. Sample 1 showed the highest average impedance while Sample 3 had the lowest average impedance. After 100 Hz, the impedance phase shows phase

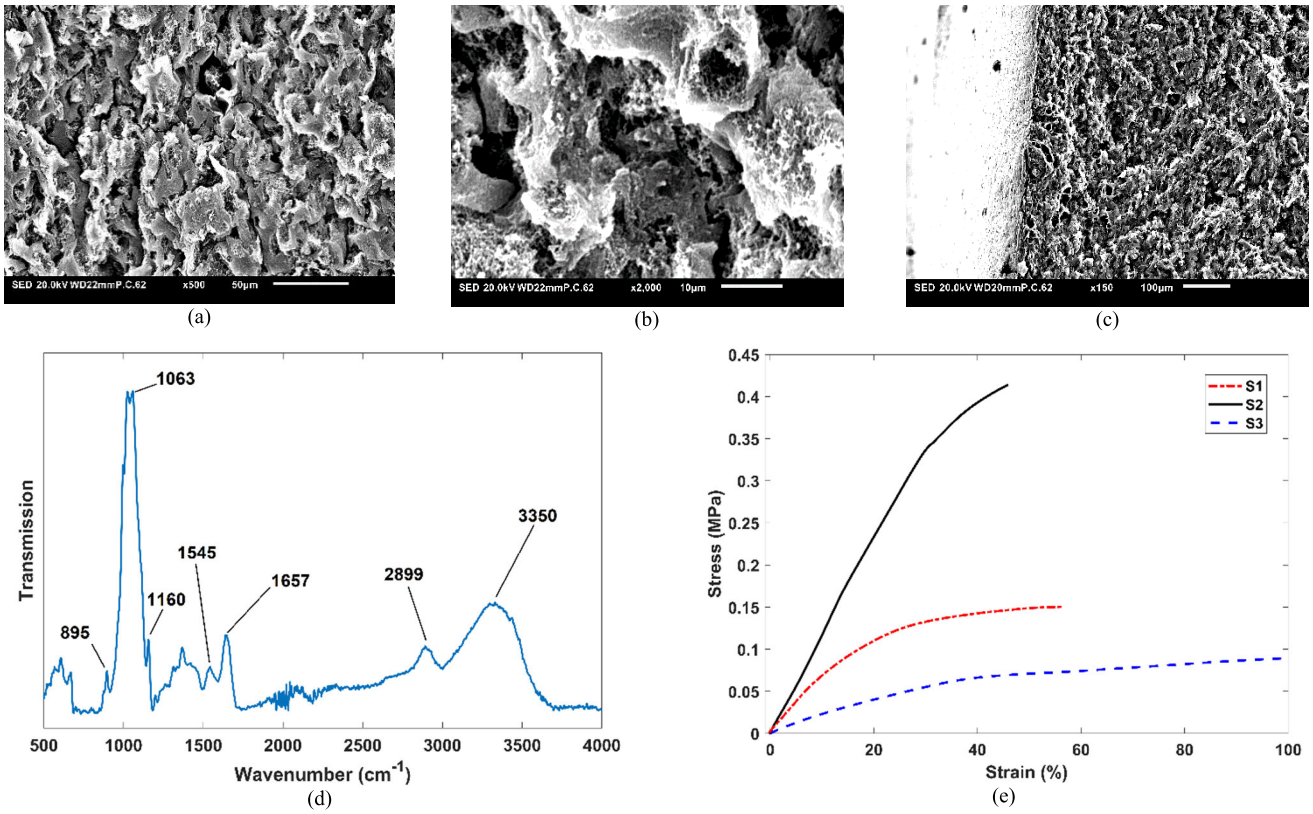

Fig. 2. Scanning electron microscope images from the cross-section of the super-critical dried porous electrode: (a) low magnification, (b) high magnification, (c) near edge cross-section view. (d) Fourier transform infrared (FTIR) spectrum of the electrode material. (e) Stress-strain curves of the wet electrode material under tensile test for three different carbon nanotube (CNT) concentrations, namely, Sample 1 (S1), Sample 2 (S2), and Sample 3 (S3) corresponding to 2wt%, 4wt%, and 6wt% CNT concentration, respectively.

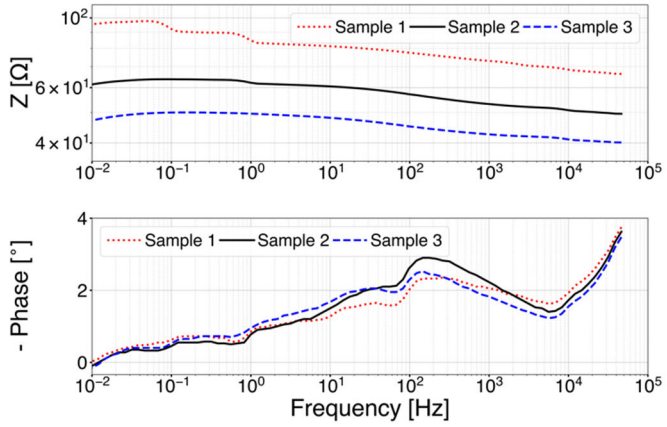

Fig. 3. Impedance magnitude (top) and phase response (bottom) of different samples of the material after being soaked in water.

TABLE I
IMPEDANCE OF THE ELECTRODES FOR THE FREQUENCY RANGE OF 0.1 HZ TO 10 KHZ

Sample	Average Impedance
1	80.8 ± 9.55 Ω
2	58.1 ± 4.89 Ω
3	46.1 ± 3.43 Ω

shifts, however, the largest shift was no more than 3°. The results of electrical characterization suggested that the wet electrode materials presented here can be useful to perform the electrical stimulation due to their low impedance in the desired frequency range [5]. We also measured the average impedance of a commercial hydrogel which was 9814.49±1297.5 Ω.

D. Electrode Cover and Packaging Design

The humidity of the environment and the ambient airflow in which the electrode is being used may highly affect the electrode's rate of drying. To increase the working time, reduce the drying rate, and improve the usability of the electrodes, we needed a cover for the electrode surfaces not in contact with human skin. The wet electrode can be cut into desired shapes and sizes and then embedded into the cover for the practical application. We propose the use of elastomeric materials, such as thermosets (rubber-based) and thermoplastic polymers to make the cover. The flexible cover would be conformal to the desired body curvature and also provide a layer of protection from unexpected mechanical loads. The back surface of the cover should serve as an electrical interface for the cabling to connect the stimulator to the electrodes. Accordingly, we have designed the cover for the two configurations used in the FES application, as shown in Fig. S2.

Fig. S2(a) shows the circular electrode packaging design where the effective diameter of the wet electrode is 25 mm. Fig. S2(b) represents the square shape electrode where the

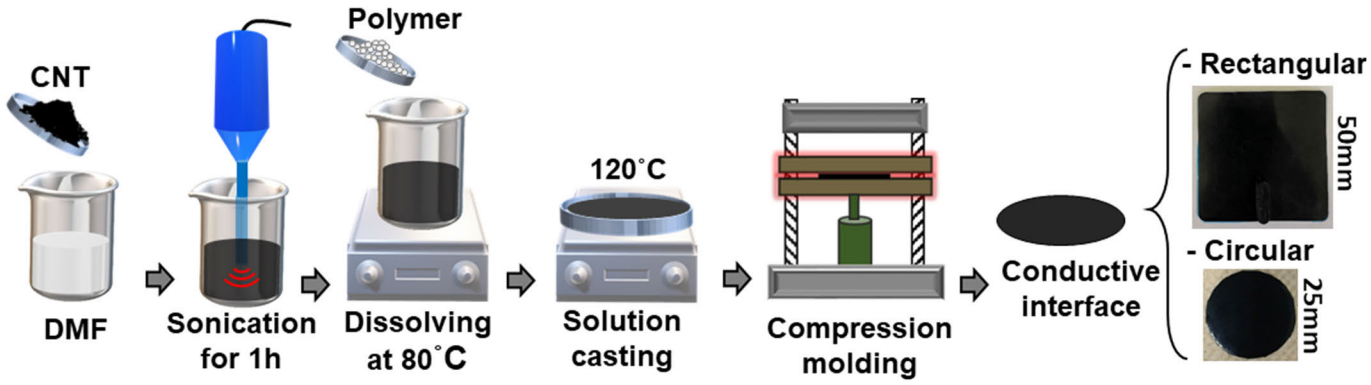

Fig. 4. Fabrication process of the conductive interface for the electrode backing.

length of side is 50 mm for the effective wet electrode contact surface. Both designs were based on the standard commercial electrode dimensions used for the FES application. For both designs, elastomeric walls were tailored from commercially available rubber-based materials (Neoprene-40A, ∼2 mm thick). Note that the walls must be electrically insulative to ensure that the electric pulses do not interfere with non-targeted locations. The elastomeric features of the walls would also act as a sealing for the wet electrode providing a plunger-like behavior for better attachment to the skin and longer water retention. The back of the design was made of a flexible thin-film polymer composite which is permanently adhered to the walls. Such thin-film had to be flexible, durable, and electrically conductive to act as the interface between the wet electrode and the stimulator connections. The connection of the stimulator wire to the electrode backing cover is shown in Fig. S2(c) for the rectangular design.

For this purpose, we proposed the use of conductive thermoplastic polymer composites which can provide all the features needed for the interface. Based on our previous experience, we used the standard solution casting process to fabricate the conductive polymer composite interface [25], [26]. The fabrication process is discussed here, as shown in Fig. 4. Accordingly, first we dispersed the conductive filler i.e., CNT (5 wt% of the polymer) into the polymer solvent i.e., DMF (93 wt% of the total solution) through a sonication process for 1 hr at 60 Watts. Then, we added the selected thermoplastic polymer pellets (PVDF) into the dispersion and mix for 4 hrs using a magnetic stirrer at 80 °C. After the full dissolution of the polymer, we casted the solution into a petri dish and dried the sample on a hot plate for 12 hrs at 120 °C. The resulting dry polymer-CNT blend was then transferred into a compression mold setup and heated at 180 °C for 6 min and then compressed into the custom-made steel molds for 3 min to obtain thin-film layers (100 μm) with the desired dimensions (circular or square shape). The samples were then cooled down in a water bath and removed from the mold. Finally, they were attached to the elastomeric walls using permanent adhesives (Loctite, supplied from McMaster-Carr, Canada). Note that the use of PVDF as the polymer matrix and CNT as the conductive filler has shown to provide suitable electrical and mechanical properties of the targeted polymer composite [25], [26]. In fact, the high electrical conductivity and uniform dispersion of the

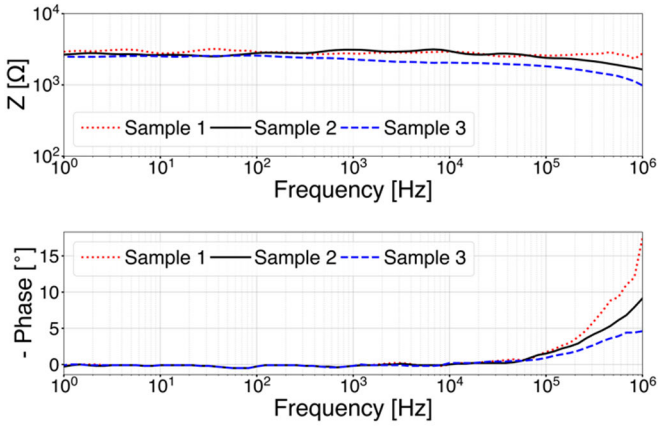

Fig. 5. Impedance magnitude and phase response of the custom cover material.

CNT into the polymer matrix provided the desired conductivity of the polymer composite, and the robustness of the selected polymers delivered a durable and flexible thin-film layer for the cover design.

To investigate the functionality of the cover design, we measured the impedance of the dry interfacial layer between the FES electrical connection and the wet electrode to ensure the desired conductivity of the layer for the signal delivery to the wet electrode through the packaging. Again, we used the electrochemical analyzer with the EIS technique. In this case, the experimental setup consisted of a two-electrode configuration with one side of the material sample connected to the working electrode, and the opposite side of the sample connected to the counter and reference electrodes. The parameters used were a sine wave with a peak amplitude of 0.005 V and a frequency range from 1 Hz to 1 MHz. For comparison, this procedure was performed on three fabricated samples with PVDF polymer matrix with the same amount of CNT (5 wt% of PVDF) for the circular shape design.

The average impedance of the PVDF-CNT samples for the frequency range tested was 2819.55 ± 176.48 Ω, 2658.49 ± 329.47 Ω, and 2167.38 ± 399.37 Ω for samples 1, 2, and 3 respectively. The values are within the same ranges and the differences could be attributed to the non-identical

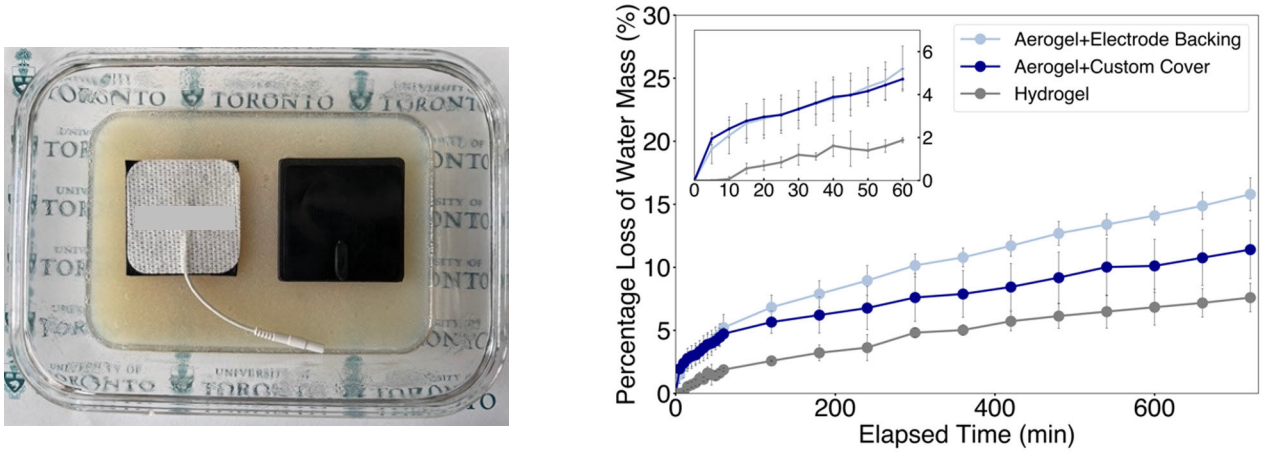

(a) (b)

Fig. 6. (a) Experimental setup to test water retention of the electrodes. On the left is the commercial hydrogel backing on top of the aerogel electrodes and on the right is the custom-made backing. (b)The percentage of water lost through time with the standard hydrogel electrode backing and the custom-made cover.

mixing process during the sonication. The impedance and phase results shown in Fig. 5 indicate that the samples own the desired properties for the range of targeted application [5]. In addition, the average sheet resistivity of the samples was measured 129.39 ± 4.41 Ω.cm (Four-point probe, Keithley 2400 SourceMeter). Therefore, the PVDF-CNT conductive polymeric film can be used as the interface between the stimulator connection and the wet electrode for FES delivery.

E. Water Drying Rate

To test the amount of water content that was lost from the samples under ambient conditions, we measured and compared the weight of the samples throughout time based on standard ISO 17617. Because the aerogel-based electrodes were kept in a wet condition before use, we measured the weight of the samples after being soaked in water for more than 24 hours and used this as the initial weight. For hydrogel electrodes, we saturated the bottom gel in water for over 24 hours as well, and used this as the initial weight. Afterwards, we placed each sample on top of an agar skin model and covered the aerogel samples with an individual backing to emulate the way they are used in the stimulation setup. We tested six aerogel-based electrode samples in total, three covered with a standard commercially available hydrogel electrode backing without the bottom gel (which was cleaned with ethanol), and three with a custom-made square cover described above. We also tested three fully saturated hydrogel electrodes. To make the agar model we used a proportion of 7g of agar-agar powder per 100 ml of solution [27]. In our case, we dissolved 14 g of agar powder in 200 ml of 0.9% saline solution, boiled it, and left it to set and cool in a glass container. The setup used can be seen in Fig. 6(a). We measured the weight of the samples every 5 minutes up to 60 minutes, and then every hour up to 12 hours to test their viability for long-term applications. We calculated the percentage of water mass loss as:

$$\frac{initial\ weight - weight\ at\ specific time}{initial\ weight} \times 100(\%) \quad (1)$$

The percentage of water weight lost through time for each backing can be seen in Fig. 6(b). With the data collected, we determined the drying rate (DR) using least squares linear regression. This is equivalent to the slope of the drying curve (in %/min), which can be expressed as: $DR = \frac{y-b}{x}$ where y is the percentage of water mass loss, b is the y-intercept (i.e., a constant), and x is the time. The hydrogel electrodes had the smallest water loss percentage, and would take the longest to fully dry out. However, we should note that the state in which we tested them would not be the way in which they are normally used. As shown in Table II, it can be noted that with the custom-made cover it would take longer for the aerogel to fully dry, and the drying rates of the aerogel samples are lower than with the hydrogel electrode backing. These results are consistent with the custom-made cover providing more insulation from ambient conditions. The aerogel samples were placed back in a water container after testing and weighed after 24 hours to verify that this process was reversible and the samples could reabsorb the lost water content. Samples under the hydrogel electrode backing fully regained their initial weight, and on average had a difference of 0.037 g less. Samples under the custom cover were also able to regain the lost water mass and on average had a difference of 0.007 g less. These results demonstrate that the electrodes could be used multiple times and could have potential for long-term use.

F. Functional Electrical Stimulation (FES) Testing

To determine the electrodes functionality during FES, we recruited twelve healthy participants (six female and six male) with a mean age of 32.42±10.37 years. The participants demographics are shown on Table III. The protocols used were approved by University Health Network's Research Ethics Board (ID#21-5298) and every participant signed an informed consent form before any of the tests took place.

To test the new aerogel electrodes, we compared both torque and comfort levels with standard self-adhesive hydrogel electrodes [28], [29]. We used the Biodex dynamometer

TABLE II
DRYING RATES FOR AEROGEL AND HYDROGEL SAMPLES 1, 2 AND 3 (S1, S2, AND S3) UNDER DIFFERENT BACKINGS

	Aerogel + Hydrogel Electrode Backing				Aerogel + Custom-Made Cover				Hydrogel			
	S1	S2	S3	Mean	S1	S2	S3	Mean	S1	S2	S3	Mean
Initial Weight [g]	4.6	4.73	4.86	4.73± 0.13	3.54	3.57	3.67	3.60± 0.06	4.74	5.04	4.58	4.79± 0.23
Drying Rate for 1 h [%/min]	0.085	0.051	0.069	0.069± 0.017	0.058	0.058	0.051	0.055± 0.004	0.030	0.034	0.030	0.032± 0.002
Drying Rate for 12 h [%/min]	0.023	0.019	0.020	0.020± 0.002	0.016	0.016	0.010	0.014± 0.003	0.009	0.011	0.012	0.011± 0.002
Estimated Drying Time to Dry 100% [h]	21.76	30.13	21.79	24.56± 4.82	29.82	24.87	29.05	27.92± 2.66	65.83	51.32	42.43	53.19± 11.81
Weight Difference after 24 h Rewetting [%]	-0.217	0	-2.058	-0.758± 1.131	0	-1.108	0.548	-0.187± 0.844	N/A	N/A	N/A	N/A

TABLE III
PARTICIPANTS DEMOGRAPHICS

Age [years]	Sex	Height [m]	Weight [kg]	Dominant Hand
57	M	1.85	94	Left
48	M	1.82	96	Right
28	F	1.65	59	Right
25	F	1.60	50	Right
28	F	1.57	48	Right
28	F	1.59	52	Right
28	M	1.82	81	Right
27	M	1.85	75	Right
25	M	1.78	70	Right
25	M	1.73	61	Right
40	F	1.65	84	Right
30	F	1.64	50	Right

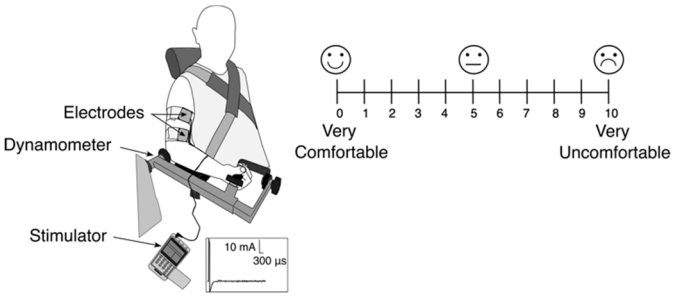

Fig. 7. The experimental setup used is shown on the left. Participants were seated and a pair of electrodes was placed on their right biceps brachii to deliver stimulation. An example of the current output from the stimulator is shown next to the stimulator. Torque was recorded from the dynamometer using a data acquisition system. On the right, the numerical rating scale printed and shown to participants during the tests where 0 was the most comfortable and 10 was the most uncomfortable.

(System 3, Biodex Medical Systems, USA) to measure the torque generated during an isometric elbow flexion.

Participants were seated on the Biodex's chair with the backrest straight. Their hand held the arm attachment's handle in a supine position and we wrapped a self-adhesive bandage around it to hold the hand in place. The armrest height was adjusted for each participant so that their shoulder would be in a comfortable neutral straight position. The dynamometer's axis of rotation was aligned to each individual's elbow. We placed two straps across their torso to maintain their position. An example of the experimental setup used is shown in Fig. 7. To record the data, we used a data acquisition system and software (LabChart, PowerLab, AD Instruments, USA). Torque was recorded at 1 kHz sampling rate. All data was collected and stored for further analysis in a computer.

We placed a pair of standard hydrogel electrodes (ValuTrode 5 × 5 cm, Axelgaard Manufacturing, Denmark) on the right biceps brachii of each participant. The anode was placed on the proximal end of the muscle (i.e., on top of the long and short heads of the brachii), while the cathode was placed on the distal end of the muscle belly. A standard hydrogel backing with the bottom gel cleaned thoroughly was used on top of the aerogel electrodes during the FES tests in order to connect them to the stimulator. The outline of the electrode placement was marked to ensure that both electrode types tested were placed in the same position. The electrodes were wrapped with self-adhesive bandages to secure them in place.

We used a portable battery-operated stimulator (EV-906, Everyway Medical Instruments, Taiwan) that is voltage-controlled with asymmetric biphasic pulses to apply the stimulation. The stimulator's parameters were set at a pulse frequency of 40 Hz, pulse width of 300 μs, and pulse amplitude dependent on each participant (8-57 mA).

We determined the sensory threshold (i.e., the amplitude when the person started feeling the stimulation), the minimum contraction threshold (i.e., mCT, amplitude when the muscle first started to twitch or contract), and the maximum tolerated contraction threshold (i.e., MTC, amplitude when the stimulation was too uncomfortable for the participant). Based on these thresholds, we calculated three different intensities (low, moderate, and high) to stimulate each participant:

$$\begin{cases} Low : mCT + 0.25 * (MTC - mCT) \\ Moderate : mCT + 0.50 * (MTC - mCT) \\ High : mCT + 0.75 * (MTC - mCT) \end{cases} \quad (2)$$

All thresholds were determined using the hydrogel electrodes, and the same intensity levels were used with both

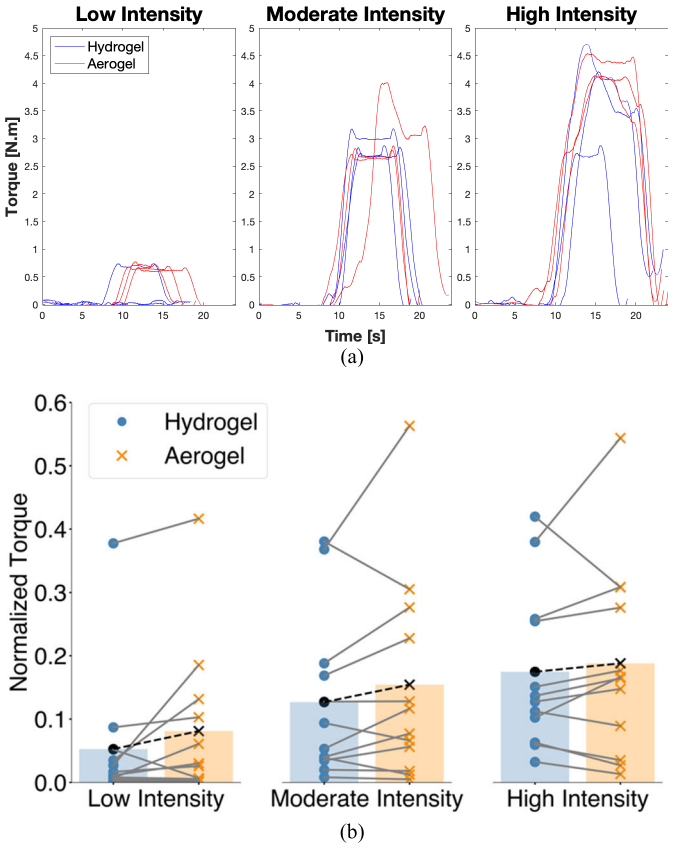

Fig. 8. (a) Sample of torque data for a participant at low, moderate and high intensity of stimulation. (b) Normalized steady-state torques for low, moderate, and high intensity stimulations.

the hydrogel electrodes and the aerogel-based electrodes. The type of electrode (i.e., new aerogel or standard hydrogel) and intensity order were randomized. Participants performed three initial voluntary contractions using their maximum effort and held each for five seconds. Then we stimulated with one type of electrode at each intensity three times. The stimulation amplitude was increased 1 mA at a time until reaching the desired intensity and held for five seconds. After each round of stimulation, participants would report verbally how comfortable the stimulation felt using a visual numerical rating scale from 0 to 10 displayed in front of them, where 0 would be very comfortable and 10 very uncomfortable, as shown in Fig. 7. Once we finished testing one type of electrode for all intensities, we changed the electrode type and repeated the same stimulation procedure described before.

After data collection, we used MATLAB (v.2021a, Mathworks, USA) to filter and analyze the data. In Fig. 8(a) we exemplify the torque values across all iterations of testing with both electrode types for a single participant. For the statistical analysis of torque and comfort rating, we used a two-sided Wilcoxon's signed-rank test.

III. Results

A. FES-Generated Torque

To compare the torque generated by each electrode type, we used the average steady-state force. The steady-state force was defined as the average force within the last second of stimulation at the desired intensity. We also used the average of the three maximum peak forces of the voluntary contractions to normalize the torque for each participant. For low intensity stimulation, the average steady-state normalized torque was 0.053±0.021 for the hydrogel electrodes, and 0.081±0.026 for the aerogel electrodes ($p = 0.117$). For moderate intensity stimulation, the average steady-state normalized torque was 0.127±0.032 for hydrogel electrodes, and 0.154±0.032 for the aerogel electrodes ($p = 0.308$). For high intensity stimulation, the average steady-state normalized torque was 0.175±0.030 for the hydrogel electrodes and 0.188±0.027 for the aerogel electrodes ($p = 0.433$). A comparison of the torque values for all intensities tested can be seen in Fig. 8(b). Compared to standard hydrogel electrodes, no statistically significant difference ($p<0.05$) was found for any of the stimulation intensities.

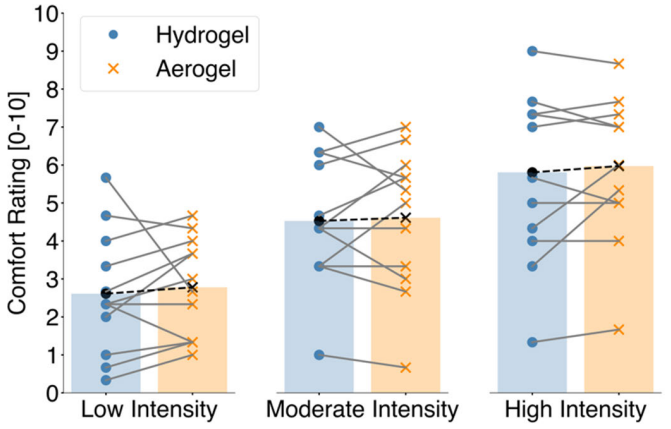

Fig. 9. Mean perceived comfort ratings for all participants at three stimulation intensities.

B. Perceived Comfort Ratings

The mean comfort rating for low intensity was 2.61±1.60 for the standard hydrogel electrodes and 2.78±1.31 for the aerogel-based wet electrodes ($p = 0.328$). For moderate intensity, comfort ratings were 4.53±1.70 for the standard hydrogel electrodes and 4.61±1.87 for the aerogel electrodes ($p = 0.683$).

For high intensity, the comfort ratings were 5.81±2.24 for standard hydrogel electrodes and 5.97±1.90 for aerogel electrodes ($p = 0.960$). The mean reported comfort ratings for each electrode type is shown in Fig. 9. No statistically significant difference ($p<0.05$) was found between both types of electrodes. For low intensity stimulation, the mean comfort ratings showed that 3 participants reported the aerogel as more comfortable, 8 participants reported the aerogel as more uncomfortable, and 1 reported the same comfort. For moderate intensity, 5 participants reported the wet aerogel as more comfortable, 5 as more uncomfortable, and 2 rated it the same as the hydrogel electrode. For high intensity, 5 participants reported the aerogel as more comfortable, 5 as more uncomfortable, and 2 rated both electrode types the same.

IV. Discussion

Hydrogel electrodes are often used as the standard in non-invasive FES therapy. Although they are practical to use, depending on each person's skin condition, the adhesive layer will start failing, and the hydrogel will start drying out with time, requiring additional tape or wrap to keep the electrodes in place. This limits their application for long-term use and for multiple reuses. Recent efforts in improving surface stimulation by replacing the existent hydrogel electrodes have aimed towards the use of textile electrodes. However these electrodes, which are inherently dry, must be used in a wet condition in order to be comfortable [8], [10], [11], [30], [31]. The constant addition of water can be considered a disadvantage for practical applications since it is a time consuming and annoying process, the stimulation sensation can be unpleasant, and the usage time of the electrodes is limited [9]. Here we presented new reusable electrodes made from an aerogel-based material which can absorb and retain a high amount of water, reducing the need for constant wetting during stimulation. These electrodes could be integrated into stimulation garments as an alternative to the textile-based electrodes which require constant wetting for a comfortable delivery of the stimulation. Due to their soft and flexible nature, they are also able to conform to different body parts easily and allow a close contact interface with the skin. These electrodes also have the advantage of being easily cut to any desired shape or size which can accommodate specific application needs. The mechanical, chemical, and electrical characterization of these aerogel-based wet electrodes showed suitable properties for stimulation purposes. To test their performance with surface stimulation, we measured the elbow joint torque during an FES induced isometric contraction at three different intensity levels and asked participants to rate how comfortable they felt each stimulation. Comparing both torque and comfort rating to those obtained with standard self-adhesive hydrogel electrodes, no statistically significant difference was found between both electrode types for either torque generated or comfort felt. However, a higher mean torque production could be observed with the aerogel electrode for all stimulation intensities tested. Although this could indicate that the proposed electrodes perform the same as standard hydrogel electrodes, the sample size of this study should be noted as a limitation. In the future, it would be beneficial to test the electrodes performance in long-term testing on individuals to see if there is a difference in their comfort level, torque production, or water retention within the span of multiple continuous hours or separate days.

V. Conclusion

In this study we have developed a new wet aerogel-based electrode which can be used for electrical stimulation. We described the fabrication process and characterized its mechanical, chemical, electrical, and water retention properties. The new electrode requires a single layer of smooth material and a custom-backing to connect it to a stimulator, and was shown to be able to retain a high content of water for long periods of time with minimal loss due to their porous hydrophilic nature. They can also be rewetted after use by soaking them in water, which allows them to return to their original saturated condition and enables reusability. Its mechanical and electrical properties were also shown to be appropriate for stimulation purposes. In comparison, the commercially available self-adhesive hydrogel electrodes use multiple different layers of material, and have an adhesive gel as an interface with the skin, which tends to lose the adhesive properties quickly, and can ultimately irritate a patient's skin. Textile electrodes, which have been made as an alternative to hydrogel electrodes, also require a wet interface which at the moment dries out within minutes. Since we tested the new electrode's performance during stimulation and found no significant difference in torque production or comfort levels compared to standard hydrogel electrodes, the aerogel-based electrodes could be integrated into garments to allow long-term use without constant rewetting. Overall, this new electrode could be used for surface electrical stimulation applications, and is a promising substitute for the existing gel-based stimulation electrodes or textile stimulation electrodes. The proposed electrode is also reusable and can retain water for long periods of time which could be beneficial for long-term applications.

Conflict of Interest

Milos R. Popovic is the Co-Founder, Director, and Shareholder in companies MyndTec Inc. and ERNE Inc., and provides consulting services to Fourier Intelligence.

References

[1] C. L. Lynch and M. R. Popovic, "Functional electrical stimulation," *IEEE Control Syst. Mag.*, vol. 28, no. 2, pp. 40–50, Apr. 2008, doi: 10.1109/MCS.2007.914689.

[2] C. Marquez-Chin and M. R. Popovic, "Functional electrical stimulation therapy for restoration of motor function after spinal cord injury and stroke: A review," *Biomed. Eng. OnLine*, vol. 19, no. 1, p. 34, Dec. 2020, doi: 10.1186/s12938-020-00773-4.

[3] N. Kapadia, B. Moineau, and M. R. Popovic, "Functional electrical stimulation therapy for retraining reaching and grasping after spinal cord injury and stroke," *Frontiers Neurosci.*, vol. 14, p. 718, Jul. 2020, doi: 10.3389/fnins.2020.00718.

[4] L. L. Baker et al. *Neuro Muscular Electrical Stimulation: A Practical Guide*, 4th ed. Downey, CA, USA: Los Amigos Research & Education Institute, 2000.

[5] T. Keller and A. Kuhn, "Electrodes for transcutaneous (surface) electrical stimulation," *J. Autom. Control*, vol. 18, no. 2, pp. 35–45, 2008, doi: 10.2298/JAC0802035K.

[6] T. Keller and A. Kuhn, "Skin properties and the influence on electrode design for transcutaneous (surface) electrical stimulation," in *Proc. World Congr. Med. Phys. Biomed. Eng.*, vols. 9–25, O. Dössel and W. C. Schlegel, Eds. Berlin, Germany: Springer, Jul. 2009, pp. 492–495, doi: 10.1007/978-3-642-03889-1_131.

[7] A. Kuhn, T. Keller, M. Lawrence, and M. Morari, "The influence of electrode size on selectivity and comfort in transcutaneous electrical stimulation of the forearm," *IEEE Trans. Neural Syst. Rehabil. Eng.*, vol. 18, no. 3, pp. 255–262, Jun. 2010, doi: 10.1109/TNSRE.2009.2039807.

[8] B. Moineau, C. Marquez-Chin, M. Alizadeh-Meghrazi, and M. R. Popovic, "Garments for functional electrical stimulation: Design and proofs of concept," *J. Rehabil. Assistive Technol. Eng.*, vol. 6, Jan. 2019, Art. no. 205566831985434, doi: 10.1177/2055668319854340.

[9] B. Moineau, M. Myers, S. S. Ali, M. R. Popovic, and S. L. Hitzig, "End-user and clinician perspectives on the viability of wearable functional electrical stimulation garments after stroke and spinal cord injury," *Disab. Rehabil., Assistive Technol.*, vol. 16, pp. 1–10, Oct. 2019, doi: 10.1080/17483107.2019.1668974.

[10] H. Zhou et al., "Stimulating the comfort of textile electrodes in wearable neuromuscular electrical stimulation," *Sensors*, vol. 15, no. 7, pp. 17241–17257, Jul. 2015, doi: 10.3390/s150717241.

[11] L. Euler, L. Guo, and N.-K. Persson, "A review of textile-based electrodes developed for electrostimulation," *Textile Res. J.*, vol. 92, nos. 7–8, pp. 1300–1320, Apr. 2022, doi: 10.1177/00405175211051949.

[12] S. G. Mosanenzadeh, Z. Saadatnia, S. Karamikamkar, C. B. Park, and H. E. Naguib, "Polyimide aerogels with novel bimodal micro and nano porous structure assembly for airborne nano filtering applications," *RSC Adv.*, vol. 10, no. 39, pp. 22909–22920, 2020, doi: 10.1039/D0RA03907A.

[13] Z. Saadatnia, S. Ghaffari Mosanenzadeh, M. Marquez Chin, H. E. Naguib, and M. R. Popovic, "Flexible, air dryable, and fiber modified aerogel-based wet electrode for electrophysiological monitoring," *IEEE Trans. Biomed. Eng.*, vol. 68, no. 6, pp. 1820–1827, Jun. 2021, doi: 10.1109/TBME.2020.3022615.

[14] S. G. Mosanenzadeh, M. Alshrah, Z. Saadatnia, C. B. Park, and H. E. Naguib, "Double dianhydride backbone polyimide aerogels with enhanced thermal insulation for high-temperature applications," *Macromolecular Mater. Eng.*, vol. 305, no. 4, Apr. 2020, Art. no. 1900777, doi: 10.1002/mame.201900777.

[15] S. Wang, A. Lu, and L. Zhang, "Recent advances in regenerated cellulose materials," *Prog. Polym. Sci.*, vol. 53, pp. 169–206, Feb. 2016, doi: 10.1016/j.progpolymsci.2015.07.003.

[16] B. P. Singh, S. Nayak, S. Samal, S. Bhattacharjee, and L. Besra, "Characterization and dispersion of multiwalled carbon nanotubes (MWCNTs) in aqueous suspensions: Surface chemistry aspects," *J. Dispersion Sci. Technol.*, vol. 33, no. 7, pp. 1021–1029, Jul. 2012, doi: 10.1080/01932691.2011.590753.

[17] H. Geng, "A one-step approach to make cellulose-based hydrogels of various transparency and swelling degrees," *Carbohydrate Polym.*, vol. 186, pp. 208–216, Apr. 2018, doi: 10.1016/j.carbpol.2018.01.031.

[18] H. Jin, Y. Nishiyama, M. Wada, and S. Kuga, "Nanofibrillar cellulose aerogels," *Colloids Surf. A, Physicochemical Eng. Aspects*, vol. 240, nos. 1–3, pp. 63–67, Jun. 2004, doi: 10.1016/j.colsurfa.2004.03.007.

[19] O. A. Tafreshi et al., "Flexible and shape-configurable PI composite aerogel films with tunable dielectric properties," *Composites Commun.*, vol. 34, Oct. 2022, Art. no. 101274, doi: 10.1016/j.coco.2022.101274.

[20] Q. Liao et al., "Flexible and durable cellulose aerogels for highly effective oil/water separation," *RSC Adv.*, vol. 6, no. 68, pp. 63773–63781, 2016, doi: 10.1039/C6RA12356B.

[21] M. Pawlaczyk, M. Lelonkiewicz, and M. Wieczorowski, "Age-dependent biomechanical properties of the skin," *Postepy Dermatol. Alergol.*, vol. 30, no. 5, pp. 302–306, Oct. 2013, doi: 10.5114/pdia.2013.38359.

[22] L. Bai et al., "Comparison of hydrophilicity and mechanical properties of nanocomposite membranes with cellulose nanocrystals and carbon nanotubes," *Environ. Sci. Technol.*, vol. 51, no. 1, pp. 253–262, Jan. 2017, doi: 10.1021/acs.est.6b04280.

[23] M. Tarfaoui, K. Lafdi, and A. El Moumen, "Mechanical properties of carbon nanotubes based polymer composites," *Composites B, Eng.*, vol. 103, pp. 113–121, Oct. 2016, doi: 10.1016/j.compositesb.2016.08.016.

[24] E. Barsoukov and J. R. Macdonald, *Impedance Spectroscopy: Theory, Experiment, and Applications*, 2nd ed. Hoboken, NJ, USA: Wiley-Interscience, 2005.

[25] M. Chu and H. E. Naguib, "Soft flexible conductive CNT nanocomposites for ECG monitoring," *Smart Mater. Struct.*, vol. 30, no. 6, Jun. 2021, Art. no. 065003, doi: 10.1088/1361-665X/abefb6.

[26] T. Chen et al., "Novel, flexible, and ultrathin pressure feedback sensor for miniaturized intraventricular neurosurgery robotic tools," *IEEE Trans. Ind. Electron.*, vol. 68, no. 5, pp. 4415–4425, May 2021, doi: 10.1109/TIE.2020.2984427.

[27] L. Beckmann et al., "Characterization of textile electrodes and conductors using standardized measurement setups," *Physiological Meas.*, vol. 31, no. 2, pp. 233–247, Feb. 2010, doi: 10.1088/0967-3334/31/2/009.

[28] M. G. Garcia-Garcia, L. I. Jovanovic, and M. R. Popovic, "Comparing preference related to comfort in torque-matched muscle contractions between two different types of functional electrical stimulation pulses in able-bodied participants," *J. Spinal Cord Med.*, vol. 44, no. sup1, pp. S215–S224, Sep. 2021, doi: 10.1080/10790268.2021.1970882.

[29] B. J. Forrester and J. S. Petrofsky, "Effect of electrode size, shape, and placement during electrical stimulation," *J. Appl. Res.*, vol. 4, no. 2, pp. 1–9, 2004.

[30] K. Yang, C. Freeman, R. Torah, S. Beeby, and J. Tudor, "Screen printed fabric electrode array for wearable functional electrical stimulation," *Sens. Actuators A, Phys.*, vol. 213, pp. 108–115, Jul. 2014, doi: 10.1016/j.sna.2014.03.025.

[31] L. Euler, L. Guo, and N.-K. Persson, "Textile electrodes: Influence of knitting construction and pressure on the contact impedance," *Sensors*, vol. 21, no. 5, p. 1578, Feb. 2021, doi: 10.3390/s21051578.